

Flammability and Dehydration of Painted Gypsum Wallboard Subjected to Fire Heat Fluxes

J. Robert McGraw, Jr.
Frederick W. Mowrer, Ph.D., P.E.
Department of Fire Protection Engineering
University of Maryland
College Park, Maryland 20742-3031

ABSTRACT

The flammability and dehydration of painted gypsum wallboard (GWB) exposed to fire heat fluxes are investigated. Painted GWB samples are subjected to constant incident heat fluxes ranging from 25 to 75 kW/m² for periods ranging from 5 to 15 minutes in the Cone Calorimeter. A number of coats of latex interior paint, including 0, 2, 4, 6 and 8 coats, are applied over a single coat of latex primer to the exposed surface of 15.9-mm (5/8-in.) thick type X GWB. A model is used to evaluate the potential for flame spread based on the Cone Calorimeter results. A two-step dehydration model based on a finite difference formulation is described for GWB. Experimental results indicate a distinct dehydration front can be observed by visual inspection; further analysis is needed to determine the composition of the GWB on each side of this front.

KEYWORDS: Cone Calorimeter, dehydration, fire model, flame spread, gypsum wallboard

NOTATION

- c Specific heat (kJ/kg-K)
 C_1 - C_5 Constants described in the text
 h_c Convective heat transfer coefficient (kW/m²-K)
 k Thermal conductivity (kW/m-K)
 k_f Linearized flame length coefficient (~ 0.01 m²/kW)
 L Heat of gasification of a material (kJ/g)
 L_v Heat of vaporization of water (kJ/g)
 $m_{H_2O}^n$ Mass of water per unit area in a node (g/m²)

| | |
|--------------------|--|
| \dot{m}''_{H_2O} | Dehydration rate per unit area (g/s-m ²) |
| \dot{q}''_{net} | Net incident heat flux to the sample per unit area (kW/m ²) |
| \dot{Q}'' | Heat release rate per unit area (kW/m ²) |
| Q'' | Heat release per unit area (kJ/m ²) |
| t_{ig} | Ignition time (s) |
| t_b | Burning duration (s) [Q''/\dot{Q}''] |
| T | Temperature (K) |
| ΔH_c | Heat of combustion for a material (kJ/g) |
| Δt | Time step (s) |
| Δx | Node thickness (m) |
| ϵ | Surface emissivity (-) |
| ρ | Density (kg/m ³) |
| σ | Stefan-Boltzmann constant (5.67×10^{-11} kW/m ² -K ⁴) |

INTRODUCTION

Over the past fifty years, painted gypsum wallboard (GWB) has become perhaps the most widely used wall and ceiling interior finish. Available in a range of standard sizes and thicknesses, GWB consists of a gypsum (*Calcium sulfate dihydrate* – CaSO₄·2H₂O) core bonded between paper facers. The paper facers provide strength and toughness, as well as a surface that is easily finished, to the relatively brittle gypsum core. The gypsum core serves as a noncombustible substrate with beneficial fire resistance properties derived from the bound water of hydration in the gypsum.

Under fire conditions, the exposed paper facer and painted finish of GWB frequently burns out locally in the vicinity of the exposure fire. Williamson, et al., [1] observed and documented this behavior while investigating ignition sources used in room fire test methods. Under some conditions, however, the finished GWB surface will propagate a fire. When this happens, a distinct spike is observed in the heat release rate as the thin combustible surface ignites then quickly burns out. The question is under what conditions painted GWB is likely to spread a fire.

Whether or not a fire spreads on the GWB surface, the gypsum core will dehydrate under fire exposure conditions. The extent of dehydration depends on the intensity and duration of the exposure. Under prolonged exposure, the GWB will fully dehydrate, leaving behind a friable residue of anhydrous calcium sulfate (CaSO₄). The dehydration process absorbs considerable heat while maintaining relatively low temperatures within and behind the GWB until the dehydration is complete. For this reason, GWB is widely used in fire resistant building assemblies [2].

Following a fire, damage patterns observed on painted GWB surfaces often are used to provide clues about the fire [3]. A technique to estimate fire severity at a particular location based on GWB damage, particularly dehydration depth, would be desirable as an aid to fire investigation and reconstruction. Experimental results and field experience indicate a distinct front can be observed by visual inspection in partially dehydrated GWB. A technique is

developed to determine the location of this front; this technique involves scoring and breaking the GWB in much the same way as it is typically cut during field installation.

In this work, the Cone Calorimeter [4] is used to investigate the flammability and dehydration of painted GWB. Painted GWB samples are subjected to incident heat fluxes ranging from 25 to 75 kW/m² for periods ranging from 5 to 15 minutes in the Cone Calorimeter. Two, four, six and eight coats of latex interior paint are applied over a single coat of latex primer to the exposed paper surface of 15.9-mm (5/8-in.) thick type X GWB. Unpainted GWB samples are also evaluated for comparison. A flame spread model, developed by Quintiere and coworkers [5-7] and previously applied to thin textiles adhered to GWB substrates [8], is used to evaluate the potential for flame spread based on the Cone Calorimeter results. Based on this analysis, the concept of a critical heat flux for upward flame spread is developed.

A two-step dehydration model for GWB is described. This model, based on an explicit finite difference formulation, has been implemented as a spreadsheet template. The user can specify a constant or variable convective-radiative boundary condition at the exposed GWB surface. The model calculates node temperatures, net heat flux to the surface, and dehydration depth histories. Model predictions of dehydration depth are compared with experimental results.

FLAME SPREAD ANALYSIS

The model used to evaluate the potential for upward flame spread on painted GWB is undergoing continued development by Quintiere and coworkers [5-7]. Based on certain simplifying assumptions, this model produces a flammability parameter, b , defined as:

$$b \equiv k_f \dot{Q}'' - t_{ig} / t_b - 1 \quad (1)$$

Acceleratory flame spread is indicated if the value of the flammability parameter is positive, decay to extinction is expected if the flammability parameter is negative, and steady spread will occur, at least in theory, if the flammability parameter evaluates precisely as zero. This flammability parameter exhibits the critical nature of upward flame spread, where small perturbations in the input parameters can result in large differences in outcome for scenarios near the critical limit. Based on this critical behavior, it is conceivable that the addition of a single coat of paint may at some point tip the balance in favor of acceleratory spread rather than localized burnout. One objective of this work was to see if such relatively fine distinctions could be discerned using the Cone Calorimeter.

Evaluation of the flammability parameter requires evaluation of the respective characteristic parameters used to calculate it. Mowrer and Williamson [8] describe a technique for using Cone Calorimeter data directly to evaluate these characteristic parameters and the associated flammability parameter for thin materials adhered to GWB substrates. For a given incident heat flux, the ignition time (t_{ig}), the peak unit heat release rate (\dot{Q}'') and the unit total heat release (Q'') are measured directly in the Cone Calorimeter and substituted into Equation 1. This technique was used to calculate the flammability parameter for the different combinations of incident heat flux and coats of paint. Results are shown in Table 1.

Representative heat release rate curves are shown in Figure 1(a) for the 50 kW/m² exposure and in Figure 1(b) for the 75 kW/m² exposure. It is noted that Dillon [9] explores a number of different techniques for deriving the characteristic parameters from Cone Calorimeter data; for GWB, these techniques do not differ significantly from the one employed here.

TABLE 1. Cone calorimeter results and calculated flame spread parameters.

| Incident Heat Flux (kW/m ²) | Coats of Paint | t _{ig} (sec) | Q̇ _{peak} (kW/m ²) | Q̇ (kJ/m ²) | t _b (sec) | b (-) | Flame Spread Indicated? |
|---|----------------|-----------------------|---|-------------------------|----------------------|-------|-------------------------|
| 25 | 0 | NI | N/A | N/A | N/A | N/A | No |
| 25 | 2 | NI | N/A | N/A | N/A | N/A | No |
| 25 | 4 | NI | N/A | N/A | N/A | N/A | No |
| 25 | 6 | NI | N/A | N/A | N/A | N/A | No |
| 25 | 8 | NI | N/A | N/A | N/A | N/A | No |
| 50 | 0 | 37 | 111 | 1561 | 14 | -2.55 | No |
| 50 | 2 | 41 | 211 | 2284 | 11 | -2.65 | No |
| 50 | 4 | 42 | 224 | 2359 | 11 | -2.69 | No |
| 50 | 6 | 44 | 240 | 2651 | 11 | -2.63 | No |
| 50 | 8 | 43 | 215 | 2366 | 11 | -2.75 | No |
| 75 | 0 | 14 | 134 | 1527 | 11 | -0.91 | No |
| 75 | 2 | 15 | 206 | 2773 | 14 | -0.06 | No |
| 75 | 4 | 16 | 210 | 2949 | 14 | -0.02 | No |
| 75 | 6 | 17 | 215 | 3318 | 16 | 0.03 | Yes |
| 75 | 8 | 9 | 214 | 3378 | 16 | 0.60 | Yes |

NI = No Ignition

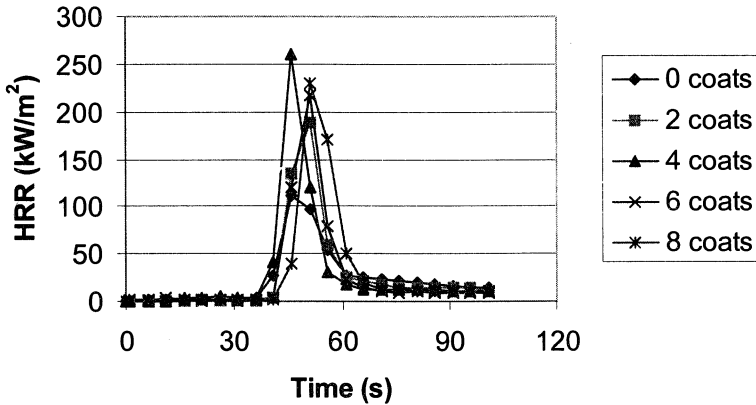


FIGURE 1(a). Representative heat release rate histories at 50 kW/m² exposure.

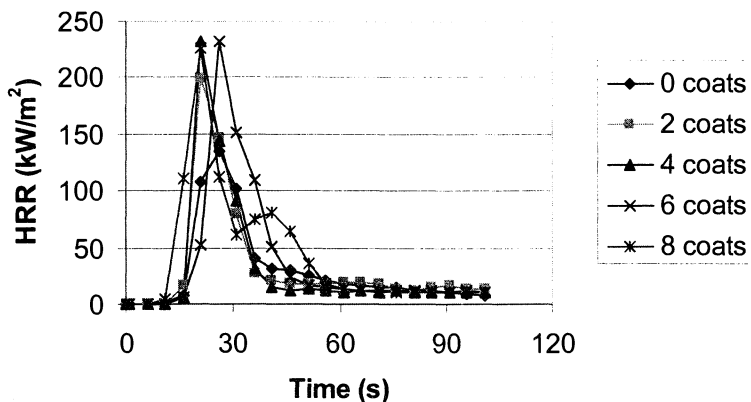


FIGURE 1(b). Representative heat release rate histories at 75 kW/m² exposure.

The painted GWB samples did not ignite at an exposure heat flux of 25 kW/m². This is consistent with reported critical heat flux values of 26-28 kW/m² for unpainted GWB [9]. When subjected to an imposed heat flux of 50 kW/m², ignition times for the painted samples ranged from 41 to 43 seconds, peak unit heat release rates ranged from 211 to 240 kW/m² and burning durations were 11 seconds. At this heat flux, the flammability parameter was always negative, with values in the range of -2.63 to -2.75, strongly suggesting that acceleratory flame spread is not likely to occur at an incident heat flux of 50 kW/m². In comparison, the unpainted sample ignited in 37 seconds at an imposed heat flux of 50 kW/m² and burned out in 14 seconds; the unpainted sample had a peak heat release rate of 111 kW/m², approximately one-half the value of the painted samples.

At an imposed heat flux of 75 kW/m², ignition times for the painted samples ranged from 15 to 17 seconds, peak unit heat release rates ranged from 206 to 215 kW/m² and burning durations from 14 to 16 seconds. At this heat flux, the flammability parameter ranged from -0.06 to +0.03; these values are near the critical limit, suggesting that acceleratory flame spread may occur at an incident heat flux of approximately 75 kW/m². The unpainted sample ignited in 14 seconds and burned out in 11 seconds at this heat flux, while achieving a peak heat release rate of 134 kW/m², resulting in a flammability parameter of -0.91.

The data suggest some interesting observations:

- In general, ignition of painted GWB was delayed slightly in comparison to unpainted GWB, with the ignition delay increasing slightly with the number of coats of paint.
- The peak heat release rate of the painted samples was approximately twice as high as that of the unpainted samples for the 50 kW/m² exposure and approximately 60% higher for the 75 kW/m² exposure.
- The total heat released by the painted samples was comparably higher than the unpainted samples. The painted samples released approximately 30% more energy at the 75 kW/m² exposure than at the 50 kW/m² exposure.

- On average, relatively small differences can be discerned in the peak heat release rates and total heat released based on the number of coats of paint, but for individual samples there is considerable scatter in the data.

Based on the experimental results, it is apparent that the potential for flame spread on painted GWB surfaces is much more sensitive to the incident heat flux at the surface than to the number of coats of paint. To evaluate the sensitivity of the flammability parameter to the imposed heat flux as well as to the number of coats of paint, the functional relationships between the parameters in Equation 1 and these two parameters are considered. Dillon [9] suggests the unit heat release rate becomes linearly dependent on the imposed heat flux as:

$$\dot{Q}'' = \dot{q}_{net}'' \frac{\Delta H_c}{L} \approx C_1 \dot{q}_{ext}'' \quad (2)$$

The ignition time is estimated based on a constant heat flux to a semi-infinite solid:

$$t_{ig} = \frac{\pi}{4} k_Q c \left[\frac{T_{ig} - T_o}{\dot{q}_{net}''} \right]^2 \approx C_2 \dot{q}_{ext}''^{-2} \quad (3)$$

The functional form of the burning duration is:

$$t_b = \frac{Q''}{\dot{Q}''} \approx \frac{Q''}{(\Delta H_c / L) \dot{q}_{net}''} \approx \frac{C_3}{C_1} \dot{q}_{ext}''^{-1} \quad (4)$$

Substituting Equations 2, 3 and 4 into Equation 1 yields:

$$b \approx k_f C_1 \dot{q}_{ext}'' - \frac{C_1 C_2}{C_3} \dot{q}_{ext}''^{-1} - 1 = C_4 \dot{q}_{ext}'' - C_5 \dot{q}_{ext}''^{-1} - 1 \quad (5)$$

Equation 5 has the form of a quadratic equation. The solution for the critical external heat flux for upward flame spread is determined by finding the solution to $b = 0$:

$$\dot{q}_{ext,crit}'' = \frac{1 \pm \sqrt{(-1)^2 - 4(C_4)(-C_5)}}{2C_4} = \frac{1 \pm \sqrt{1 + 4(C_4)(C_5)}}{2C_4} \quad (6)$$

Since C_4 and C_5 are always positive, the term within the square root operator will always have a value greater than unity. Consequently, the only valid solution to the quadratic equation is:

$$\dot{q}_{ext,crit}'' = \frac{1 + \sqrt{1 + 4(C_4)(C_5)}}{2C_4} \quad (7)$$

An example is illustrative. Assume the incident heat flux at the surface is due only to the external heat flux. Based on the data in Table 1, the value for C_1 is calculated using Equation 2 to be between approximately 3 and 5; a value of 4 is selected for this example. Based on

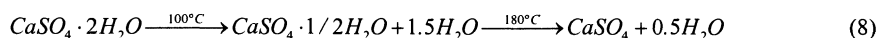
the ignition data reported in Table 1, the value for C_2 , a modified thermal response parameter [10], is approximately 100,000 for the painted GWB samples. The value for C_3 , which is the total heat release per unit area, is approximately 2,500. Using these values, the value of C_4 is 0.04 and the value of C_5 is 160, from which the critical heat flux for upward flame spread is calculated using Equation 7 to be 77 kW/m^2 . This is consistent with the experimental results, where an imposed heat flux of 75 kW/m^2 was found to be near the critical value.

So far, the analysis has not addressed potential changes in incident heat flux in the flame region, above the pyrolysis zone. Tu and Quintiere [11] suggest that wall flames typically generate heat fluxes of approximately 30 kW/m^2 in this region. Consequently, it can be argued that the characteristic ignition time in Equation 1 should be based on the ignition time associated with a heat flux of approximately 30 kW/m^2 , while the characteristic unit heat release rate and burning duration should be associated with the incident exposure fire heat flux. Mowrer and Williamson [8] found this approach to yield the most consistent results for textile wall coverings adhered to GWB substrates.

DEHYDRATION ANALYSIS

The inherent fire resistance of GWB stems from its chemical composition. Each molecule of calcium sulfate dihydrate ($\text{CaSO}_4 \cdot 2\text{H}_2\text{O}$) forming the gypsum contains two molecules of water that must be evaporated before the material's temperature can continue to increase. A literature review was performed to identify previous efforts to model the dehydration in GWB assemblies when exposed to heated environments. The models reviewed employ single-step finite difference methods to simulate the dehydration process [12-14]. These models do not account explicitly for the dehydration process that occurs when calcium sulfate dihydrate loses 1.5 moles of water to become calcium sulfate hemihydrate ($\text{CaSO}_4 \cdot 1/2\text{H}_2\text{O}$) between the temperatures of 80° and 120°C [13]. The complete dehydration follows as the material's temperature increases, producing anhydrous calcium sulfate (CaSO_4) by the time the sample temperature reaches 200°C [15]. Some models include the heat of vaporization of the water in the specific heat term for the gypsum; some also include consideration of the wood [12] or steel [11, 13] studs in the assembly.

A dehydration model was developed and implemented as a spreadsheet template. This model considers the dehydration process explicitly as a two-step process:



A one-dimensional finite difference model was developed to calculate the heating and dehydration of GWB. A flowchart of the model logic is shown in Figure 2. At the exposed surface node, the boundary condition is:

$$\rho c \frac{\partial T}{\partial t} \Big|_{x=0} = \dot{q}_{ext}'' + h_c(T_a - T_s) + \varepsilon\sigma(T_a^4 - T_s^4) + k \frac{\partial T}{\partial x} \Big|_{x=0} \quad (9)$$

In difference form, this becomes:

$$T_s(t + \Delta t) = T_s(t) + \frac{2\Delta t}{\rho c \Delta x} \left[\dot{q}_{ext}'' + h_c(T_a - T_s) + \varepsilon \sigma(T_a^4 - T_s^4) - k \frac{(T_s - T_1)}{\Delta x} \right] \quad (10)$$

At interior nodes, the energy balance during the heating stages is expressed as:

$$\rho c \frac{\partial T}{\partial t} = -k \frac{\partial^2 T}{\partial x^2} \quad (11)$$

In difference form, this becomes:

$$T_n(t + \Delta t) = T_n(t) + \frac{k\Delta t}{\rho c \Delta x^2} [T_{n+1}(t) - 2T_n(t) + T_{n-1}(t)] \quad (12)$$

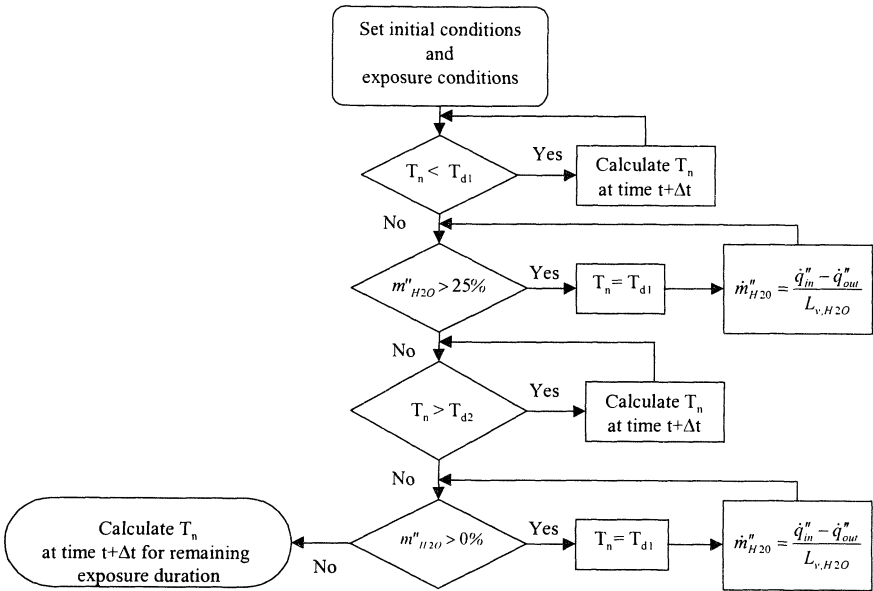


FIGURE 2. Flow chart of dehydration model.

A number of back face boundary conditions have been considered, including adiabatic, convective and conductive. For comparison with the Cone Calorimeter results, a conductive boundary condition is used to simulate the contact between the back face of the GWB and the ceramic fiber insulation material in the sample holder:

$$\rho c \frac{\partial T}{\partial t} \Big|_{x=L} = -k_{GWB} \frac{\partial T}{\partial x} \Big|_{GWB} + k_{INS} \frac{\partial T}{\partial x} \Big|_{INS} \quad (13)$$

In difference form, this can be expressed as:

$$T_L(t + \Delta t) = T_L(t) + \frac{2k_{GWB}\Delta t}{\rho c \Delta x^2} \left[T_{L-1}(t) - T_L(t) + \left(\frac{k_{INS}\Delta x_{GWB}}{k_{GWB}\Delta x_{INS}} \right) (T_{L+1}(t) - T_L(t)) \right] \quad (14)$$

When a node within the GWB reaches one of the two dehydration temperatures, $T_{d1} = 100^\circ\text{C}$ or $T_{d2} = 180^\circ\text{C}$, the absorbed heat causes evaporation of the bound moisture rather than sensible heating until the respective dehydration process is complete. This is considered by holding the node temperature constant at the respective dehydration temperature and replacing the left-hand side of Equations 9, 11 and 13 with an expression for the evaporation rate at the dehydration front:

$$\dot{m}_{H_2O}^* L_v \quad (15)$$

A value of 2,260 kJ/kg has been used for the latent heat of vaporization of water, but other values can be specified in the model. The total mass of water dehydrated from the GWB is calculated with a simple Euler equation:

$$m_{H_2O}^*(t + \Delta t) = m_{H_2O}^*(t) - \dot{m}_{H_2O}^* \Delta t \quad (16)$$

When this mass of dehydrated water reaches the respective limits of 75% and 100% of the total bound water mass for the two dehydration processes, then the calculations revert to the heating calculations, as illustrated in Figure 2. Constant material properties are assumed for each stage of dehydration; material properties used at each stage are summarized in Table 2.

TABLE 2. Material properties used for GWB dehydration model.

| Material | Conductivity, k (kW/mK) | Density, ρ (kg/m ³) | Specific heat, c_p (kJ/kg K) |
|------------------------|----------------------------|---|-----------------------------------|
| $CaSO_4 \cdot 2H_2O$ | 1.7e-4 | 700 | 1.5 |
| $CaSO_4 \cdot 1/2H_2O$ | 1.4e-4 | 598 | 1.0 |
| $CaSO_4$ | 1.3e-4 | 564 | 0.8 |

Moisture migration and condensation are not considered in the model; water evaporated in the dehydration process is assumed to leave the GWB through the exposed face without any additional impact on heat or mass transfer processes. In reality, some fraction of evaporated moisture will also move from the dehydration front towards the back face of the gypsum. As it reaches cooler regions of the GWB, this moisture will recondense, releasing the heat of vaporization in the process. On a global basis, the net effect of this evaporation-condensation cycle should be nil, but it may influence the rate of propagation of the dehydration front. Model predictions of dehydration depth are compared with experimental results in Figure 3.

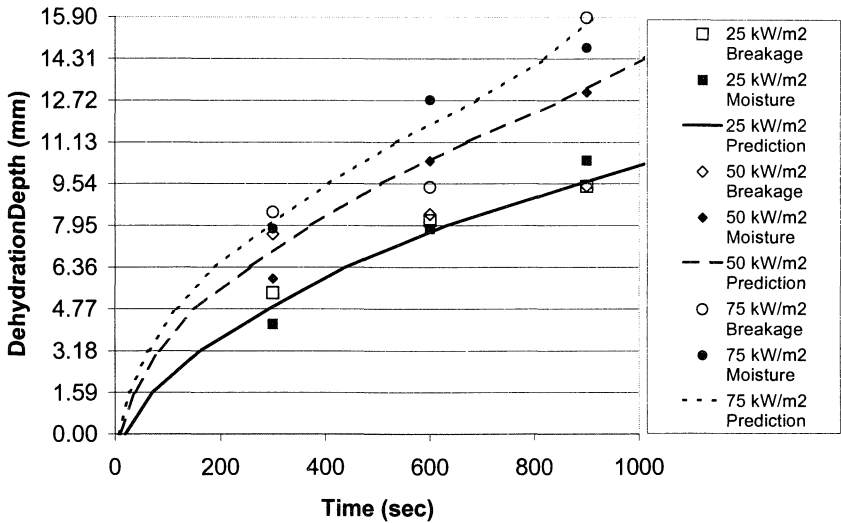


FIGURE 3. Predicted and measured dehydration depths.

Experimental results were evaluated in two ways: by cracking of the samples and by mass loss of the samples. These are identified as "Breakage" and "Moisture" in Figure 3. Following testing in the Cone Calorimeter, the samples were allowed to cool, then they were cracked in half to permit observation and measurement of the dehydration depth. The samples were broken by scoring them with a sharp blade near the center of the back face, then snapping the sample in half. This is the same process typically used to cut GWB for installation in the field. Most of the samples exhibited a distinct ridge or fracture line at a fairly uniform depth across the sample when broken. This ridge or line is believed to represent the location of the dehydration front. Samples exposed to the highest heat flux for the longest duration did not exhibit this demarcation, probably due to complete dehydration.

Dehydration depth was also inferred from mass loss data. The total mass loss was measured during and after each Cone Calorimeter test. An estimated fraction of this total mass loss was attributed to the painted paper surface, with the remaining mass loss attributed to dehydration. The dehydration depth was then calculated based on the estimated dehydration mass loss by assuming complete dehydration up to the dehydration front and no dehydration beyond. Because the painted surfaces remained virtually intact for the samples exposed to the 25 kW/m² heat flux, a relatively low fraction of mass loss was attributed to surface degradation for these samples. At the higher heat fluxes, the surfaces ignited and burned, leaving fewer residues, so a higher fraction of mass loss was attributed to the painted paper surface. This method of analysis produced results more consistent with the predictions than did the breakage data over the full range of exposure conditions and durations.

SUMMARY AND CONCLUSIONS

This investigation suggests that upward flame spread is not likely on latex-painted gypsum wallboard at incident heat fluxes of 50 kW/m^2 or less, while flame spread may occur at heat fluxes of 75 kW/m^2 or higher. The effects of preheating, as might occur in a room fire, have not been investigated directly, but these effects might be considered through appropriate adjustments in the ignition time used in Equation 1.

Based on the data obtained to date, it is not possible to distinguish a significant difference in flame spread propensity based on the number of coats of paint. Because the GWB has a paper facer that contributes significantly to the heat release, each additional coat of paint contributes relatively little to the total heat release and the burning duration. The incident heat flux has much more of an influence on the potential for flame spread than does the number of coats of latex paint, at least over the number of coats investigated. Work is continuing to investigate the effects of additional coats of paint on the propensity for flame spread on GWB. In the future, oil-based paints will be investigated to determine if similar results are obtained.

The numerical heat transfer and dehydration model developed provides a method for predicting the dehydration depth as a function of time for GWB samples. This model does a reasonably good job of tracking the dehydration of GWB when compared with mass loss measurements. A potential field method for evaluating dehydration depth based on scoring and breaking GWB specimens yielded less consistent results than the mass loss data, as indicated in Figure 3, particularly at the higher heat fluxes. The efficacy of this field method will be explored further in the future.

ACKNOWLEDGEMENTS

This work has been supported in part by grants from the Building and Fire Research Laboratory of the National Institute of Standards and Technology and from the Educational and Scientific Foundation of the Society of Fire Protection Engineers. The authors gratefully acknowledge this support.

REFERENCES

1. Williamson, R.B., Revenaugh, A., and Mowrer, F.W., "Ignition Sources in Room Fire Tests and Some Implications for Flame Spread Evaluation," in Fire Safety Science - Proceedings of the Third International Symposium, eds. G. Cox and B. Langford, pp. 657-666, Elsevier, London, 1991.
2. Gypsum Association, Fire Resistance Design Manual, 10th Edition, 60 p. April 1983.
3. Guide for Fire and Explosion Investigations, NFPA 921, National Fire Protection Association, 1995.

4. Standard Method of Test for Heat and Smoke Release Rates for Materials and Products Using an Oxygen Consumption Calorimeter, NFPA 264, National Fire Protection Association, 1995.
5. Saito, K., Quintiere, J.G., and Williams, F.A., "Upward Turbulent Flame Spread," in Fire Safety Science - Proceedings of the First International Symposium, eds. C.E. Grant and P.J. Pagni, pp. 75-86, Hemisphere, Washington, DC, 1986.
6. Cleary, T.G., and Quintiere, J.G., "A Framework for Utilizing Fire Property Tests," in Fire Safety Science - Proceedings of the Third International Symposium, eds. G. Cox and B. Langford, pp. 647-656, Elsevier, London, 1991.
7. Quintiere, J.G., "A Simulation Model for Fire Growth on Materials Subject to a Room/Corner Test," Fire Safety Journal, Vol. 18, 1992.
8. Mowrer, F.W., and Williamson, R.B., "Flame Spread Evaluation for Thin Interior Finish Materials," in Fire Safety Science - Proceedings of the Third International Symposium, eds. G. Cox and B. Langford, pp. 689-698, Elsevier, London, 1991.
9. Dillon, S.E., "Analysis of the ISO 9705 Room/Corner Test: Simulations, Correlations, and Heat Flux Measurements," M.S. Thesis, Department of Fire Protection Engineering, University of Maryland, College Park, Maryland, August 1998.
10. Tewarson, A., "Generation of Heat and Chemical Compounds in Fires," SFPE Handbook of Fire Protection Engineering (2nd ed), ed. P.J. DiNenno, National Fire Protection Association, 1995.
11. Tu, K. M. and Quintiere, J. G., "Wall Flame Heights With External Radiation," Fire Technology, 27: 3, 195-203, August 1991.
12. Cooper, L.Y., "The Thermal Response of Gypsum/Steel-Stud Wall Systems Exposed to Fire Environments – A Simulation for Use in Zone-Type Fire Models," NISTIR 6027, National Institute of Standards and Technology, Gaithersburg, MD, 1997.
13. Mehaffey, J.R., Cuerrier, P., and Carisse, G., "A Model for Predicting Heat Transfer through Gypsum-Board/Wood-Stud Walls Exposed to Fire," Fire and Materials, 18, 297-305, 1994.
14. Sultan, M.A., "A Model for Predicting heat Transfer Through Noninsulated Unloaded Steel-Stud Gypsum Board Wall Assemblies Exposed to Fire," Fire Technology, 32: 3, 239-259, August/September 1996.
15. King, G. A., Beretka, J., and Ridge, M.J., "Chemical Changes in Slabs of Cast Gypsum during Standard Tests of Resistance to Fire," Journal of Applied Chemistry and Biotechnology, 21, 159-162, June 1971.